Results in Chemistry 16 (2025) 102422

Contents lists available at ScienceDirect

Results in Chemistry

journal homepage: www.sciencedirect.com/journal/results-in-chemistry

Computational insights into the anti-diabetic potential of *Albizia antunesiana* (Mimosaceae) metabolites: A molecular docking, drug-likeness and ADMET analysis

Bitwell Chibuye [a,b,c,*], Indra Sen Singh [b], Luke Chimuka [c], Mokgaetji Monyai [c], Maseka Kenneth Kakoma [b]

[a] Department of Chemistry, Mukuba University, PO Box 20382, Itimpi Campus, Kitwe, Zambia
[b] Department of chemistry, School of Mathematics and Natural Sciences, The Copperbelt University, PO box 21692, Kitwe, Zambia
[c] Molecular Sciences Institute, School of Chemistry, University of Witwatersrand, Johannesburg, South Africa

ARTICLE INFO

Keywords:
ADMET analysis
Albizia antunesiana
Antidiabetic
Druglikeness
In silico molecular docking
Medicinal chemistry, traditional medicine

ABSTRACT

Diabetes is a complex health issue that is rapidly spreading worldwide. As a complex chronic condition, it requires continued endeavor to innovate more effective drugs. This study evaluates the antidiabetic potential of seven metabolites from the root of *Albizia antunesiana* (Mimosaceae) using molecular docking, and ADMET (Absorption, Distribution, Metabolism, Excretion, and Toxicity) analysis. The three-dimensional crystal structure of human SGLT2-MAP17 complex with Empagliflozin (PDB ID: 7VSI) was retrieved from the Protein Data Bank. Docking results showed L1 (8-Prenylnaringenin), L4 (8,8-dimethyl-2,10-dioxo-9H-pyrano[2,3-*f*]chromen-9-yl) *(Z)*-2-methylbut-2-enoate), and L7 (4-sulfophenyl)octanoic acid) had favorable binding energies comparable to the reference antidiabetic drug, Empagliflozin. ADMET profiles indicated high gastrointestinal absorption and favorable drug-likeness for most metabolites. Toxicity analysis revealed L2 (5,6,2′-Trimethoxyflavone) and L3 (Emodic acid) as the safest candidates, with low toxicity risks for hepatotoxicity, carcinogenicity, and nephrotoxicity. L2 and L3 were identified as promising drug candidates based on their overall pharmacokinetic and toxicity profiles, suggesting potential candidates for further development as antidiabetic agents. Furthermore, molecular dynamics analysis indicated that L3 exhibited favorable dynamic behavior.

1. Introduction

Traditional medicine has long been a cornerstone of healthcare in many regions of the world, offering a rich repository of botanical remedies utilized for the treatment of various diseases. Among these, the plant *Albizia antunesiana*, a member of the Mimosaceae family, has been employed in traditional medicine in Zambia for its purported therapeutic properties. Medicinal plants from the Mimosaceae family, recognized for their diverse medicinal uses, have garnered attention for their potential efficacy in managing diabetes, a condition that poses a significant health burden globally [1]. Diabetes mellitus, characterized by chronic hyperglycemia resulting from defects in insulin secretion, insulin action, or both, remains a major health challenge [2,3]. The management of diabetes traditionally relies on pharmacological and lifestyle interventions, with a growing interest in natural products offering additional therapeutic options.

A. antunesiana has been used in traditional Zambian medicine as a remedy for diabetes, yet scientific validation of its efficacy and safety is limited. This study aims to bridge this gap by providing a scientific basis for the traditional use of *A. antunesiana* in diabetes treatment. QuEChERS (Quick, Easy, Cheap, Effective, Rugged, and Safe) extraction method was used to obtain metabolites from the root samples of the plant [4]. Following extraction, liquid chromatography coupled with mass spectrometry (LCMS2) and the GNPS (Global Natural Products Social) networking tool was used to identify the metabolites present in the root extract [5]. The analysis led to the tentative identification of 58 metabolites, shedding light on the chemical complexity of *A. antunesiana* and its potential bioactive compounds.

By elucidating the metabolite profile of the root of *A. antunesiana*, this study not only supports its traditional use but also lays the groundwork for future research into its role as a natural antidiabetic remedy. The findings from the current study contribute to the broader

* Corresponding author at: Department of Chemistry, Mukuba University, PO Box 20382, Itimpi Campus, Kitwe, Zambia.
E-mail address: bchibuye@mukuba.edu.zm (B. Chibuye).

https://doi.org/10.1016/j.rechem.2025.102422
Received 22 December 2024; Accepted 3 June 2025
Available online 4 June 2025

understanding of plant-based treatments and their integration into modern therapeutic practices. This research involves an in silico analysis of anti-diabetic potential through molecular docking, with the assessment of physicochemical properties and drug-likeness, for seven metabolites derived from the root of the medicinal plant, *A. antunesiana*.

The study is exclusively based on computational models and predictions. The study uses Empagliflozin as reference drug. Empagliflozin, a safe and well-established drug is a key treatment option for managing diabetes and related conditions. Its ability to efficiently control blood glucose levels and its mild blood pressure-lowering effects make it a promising medication. It holds potential as a valuable treatment for patients from various backgrounds suffering from Type 2 diabetes and cardiovascular diseases [6]. The encouraging results of this study indicate a clear need for further experimental validation to verify the anti-diabetic activities. Hence, future work should incorporate in vitro or in vivo experiments to further elucidate the anti-diabetic effects of the selected metabolites of this study.

2. Materials and methods

2.1. Identification of ligands using GNPS

For bioactive metabolite annotation, the MS2 Bruker raw data file was used to tentatively identify metabolites using the molecular networking tool GNPS through two standard workflows as described by Chibuye et al. (2024) [7], with modifications as depicted in Fig. 1.

Fifty eight (58) metabolites were tentatively identified and are shown in Table S1. Some metabolite features such as cosine, *m/z* error, mass difference, precursor m/z, and MS2 fragmentation are shown. The annotated metabolites are also available online at: https://gnps.ucsd.edu/ProteoSAFe/result.jsp?task=a9e931c3021b4d13922ba1564a0f8f7b&view=group_by_compound

2.2. Selection of metabolites for docking study

Seven ligand molecules (Fig. 2) were selected from the phytochemicals identified in the root of *A. antunesiana*, as listed in Table S1. These phytochemicals were tentatively identified through mass spectrometry and molecular networking tools. Future research should consider employing techniques such as Nuclear Magnetic Resonance (NMR) to

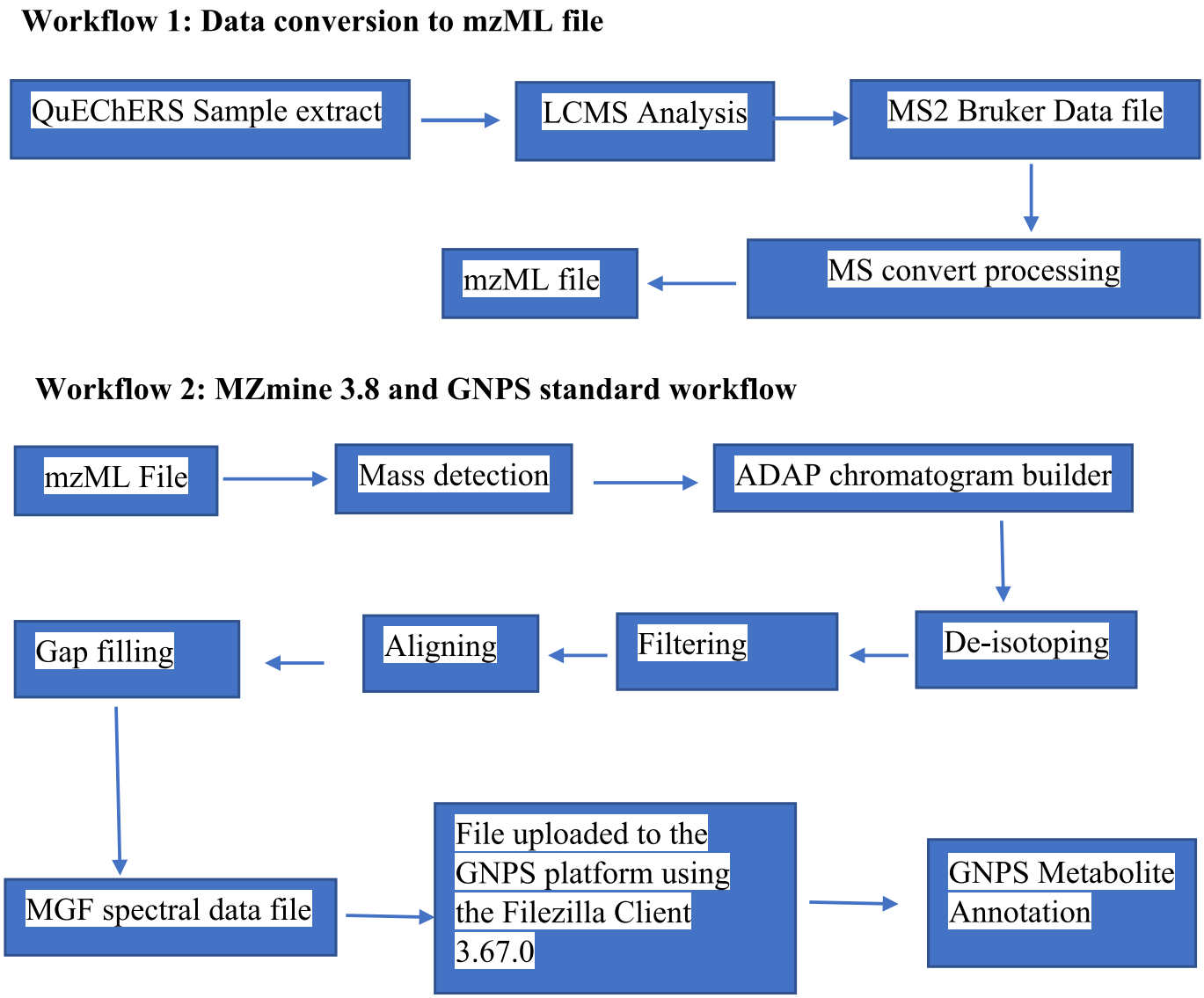

Fig. 1. LCMS2 –GNPS workflows for tentative metabolite annotation.

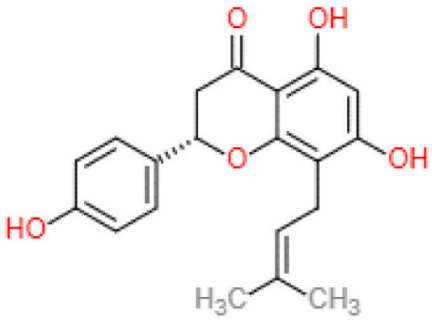

L1 (8-Prenylnaringenin)

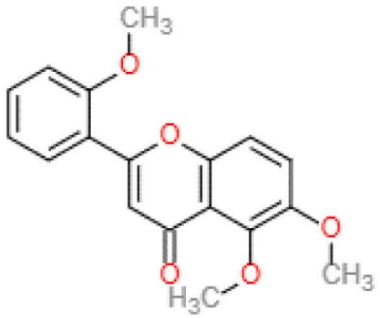

L2 (5,6,2'-Trimethoxyflavone)

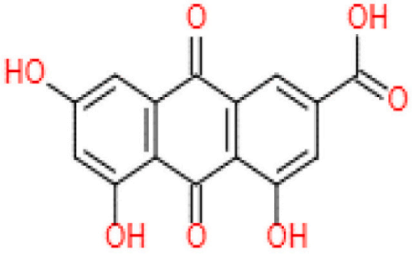

L3 (Emodic acid)

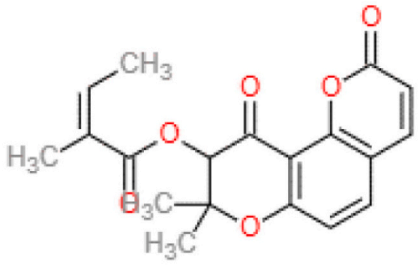

L4 (8,8-dimethyl-2,10-dioxo-*9H*-pyrano[2,3-*f*]chromen-9-yl) *(Z)*-2-methylbut-2-enoate)

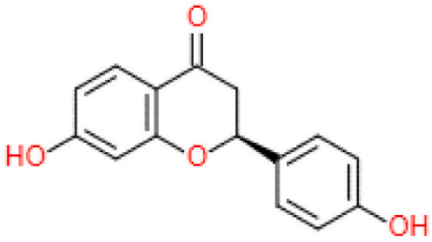

L5 *(2S)*-7-hydroxy-2-(4-hydroxyphenyl)-2,3-dihydrochromen-4-one)

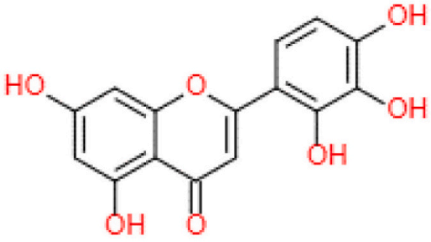

L6 (5,7-dihydroxy-2-(2,3,4-trihydroxyphenyl)chromen-4-one)

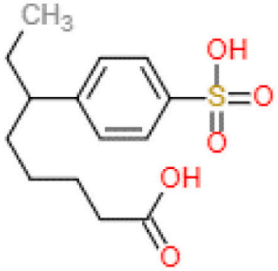

L7 (6-(4-sulfophenyl)octanoic acid)

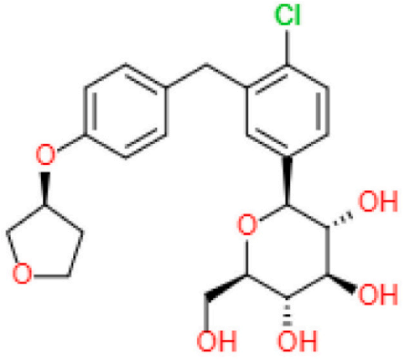

L8 (Empagliflozin - Reference antidiabetic drug)

Fig. 2. The seven metabolites selected from the root of *A. antunesiana* as potential antidiabetic drug candidates, alongside the reference drug, empagliflozin.

further confirm the characterization of these metabolites. The selection of these seven metabolites, out of a total of 58 was justified based on their binding energies, which were less than −5 kcal/mol, and their compliance with the Lipinski rule, a key criterion for medicinal compounds [8]. Additionally, assessments using www.swissadme.ch and https://ox-new.charite.de/protox indicated that the selected metabolites exhibited better ADMET (Absorption, Distribution, Metabolism, Excretion, and Toxicity) properties compared to the other metabolites. The ligand molecules, L1 (8-Prenylnaringenin), L2 (5,6,2′-Trimethoxyflavone), L3 (Emodic acid), L4 (8,8-dimethyl-2,10-dioxo-9H-pyrano

[2,3-*f*]chromen-9-yl) *(Z)*-2-methylbut-2-enoate), L5 (2*S*)-7-hydroxy-2-(4-hydroxyphenyl)-2,3-dihydrochromen-4-one), L6 (5,7-dihydroxy-2-(2,3,4-trihydroxyphenyl)chromen-4-one), L7 (6-(4-sulfophenyl)octanoic acid) and the reference drug, L8 (Empagliflozin) are shown in Fig. 2.

2.3. Justification for selection of empagliflozin as a reference antidiabetic drug

Choosing empagliflozin as a reference antidiabetic drug in the current study is well justified for several reasons. Firstly, empagliflozin functions as SGLT2 (sodium-glucose co-transporter 2) inhibitor, effectively lowering blood glucose levels by promoting glucosuria [9]. This established mechanism of action provides a clear target for identifying new antidiabetic compounds with similar or complementary effects. Moreover, empagliflozin has demonstrated significant efficacy in clinical trials, notably the EMPA-REG OUTCOME trial, where it not only lowered blood glucose levels but also reduced the risk of cardiovascular events in patients with type 2 diabetes [10]. Its proven benefits position it as a robust benchmark for assessing the efficacy of newly discovered metabolites. Additionally, empagliflozin features a relatively favorable safety profile compared to some other antidiabetic medications [11,12]. This aspect is crucial in computational studies since both efficacy and safety need to be evaluated for any new drug candidates derived from plant sources. Furthermore, comprehensive pharmacokinetic and pharmacodynamic data on empagliflozin are readily available, facilitating accurate computational modeling and simulations [13]. It was thus hoped that this study would leverage this rich dataset to make comparisons with the selected potential candidates, enhancing the robustness of the findings.

2.4. Identification of target protein and prediction of binding sites for docking analysis

The three-dimensional crystal structure of human SGLT2-MAP17 complex with Empagliflozin (PDB ID: 7VSI) was retrieved from the Protein Data Bank (http://www.pdb.org). The docking study involved identifying the active binding sites of the protein, which was achieved using the CASTp and COACH servers [7]. These tools facilitate the identification of both accessible surface pockets and inaccessible internal cavities, providing detailed information on the size and characteristics of these sites for proteins and other molecules.

2.5. Molecular docking analysis

Docking simulations were performed using AutoDock Tools. The selected ligand molecules and the reference drug were docked to human protein, SGLT2-MAP17 (PDB ID: 7VSI), with the protein treated as a rigid body and the ligands allowed flexibility. Each docking experiment comprised 10 runs, with 150 individuals and 500,000 energy evaluations using the Lamarckian Genetic Algorithm (LGA) [7,14]. This validated algorithm efficiently balances systematic search and computational demand to explore ligand-protein conformation space. The specified energy scores and population size ensured the exploration of conformational space and identified the optimal binding position of the ligands. The search grid extended 70 points per dimension with a step size of 0.375 Å, centered on the protein's binding site. AutoDock results provided insights into the binding positions, conformations of the active sites, and interaction estimations. The docked conformation with the lowest binding energy was selected to analyze the binding mode. Typically, the best docked conformation is determined by the lowest binding energy (> -5 kcal), which often correlates with biologically relevant interactions [7,14]. Hydrogen bonds and other interactions within the ligand-protein complex were analyzed using the Discovery Studio 2021 Client molecular viewer.

2.6. ADMET analysis: Evaluating pharmacodynamics properties

ADMET analysis is essential for determining pharmacodynamics properties of a molecule. Using the web-based platform SWISSADME (www.swissadme.ch/; last accessed on 15 October 2024), the ADMET properties of pharmaceuticals and natural bioactive metabolites were assessed for their best matches [15]. Ligand SMILES structures retrieved from PubChem were submitted to SWISSADME for this evaluation.

2.7. Toxicity assessment using ProTox-II

Toxicity of the metabolites was analyzed and predicted using the online web tool ProTox-II (https://ox-new.charite.de/protox; accessed on 8 August 2024).

3. Results and discussion

3.1. Evaluation of in silico antidiabetic activity

In silico docking study was performed to assess the inhibitory potential of specific metabolites on the target protein 7VSI. The findings of the molecular docking analysis are summarized in Table 2 and depicted in Figs. 3 and S1. Table 2 includes data on intermolecular energy, binding energy, binding affinity, inhibition constant, and ligand efficiency. Interacting residues, their types, and distances are detailed in Table S2.

Fig. 3 is the best docked complex showing 2D and 3D interactions of L7 (6-(4-sulfophenyl)octanoic acid) metabolite with the 7VSI receptor. Fig. S1 illustrates the 2D and 3D interaction complexes of the ligands (L1, L2, L3, L4, L5, L6 and L8) with the 7VSI receptor.

3.1.1. Discussion of in silico molecular docking

The molecular docking study provided significant insights into the binding affinities and inhibitory potentials of various ligands compared to Empagliflozin. The results demonstrate a range of interactions between the selected metabolites and the 7VSI protein target, with some ligands displaying potential to be effective antidiabetic agents.

The top-performing compound, L7 (6-(4-sulfophenyl)octanoic acid), exhibited the most favorable interaction profile with the lowest intermol energy (−10.27 kcal/mol) and the lowest inhibition constant (4.54 μM). These parameters suggest that L7 has a stronger affinity for the target protein than Empagliflozin, which had an inhibition constant of 10.04 μM. Lower inhibition constants indicate better inhibitory potential, and L7's performance suggests it could be highly effective in inhibiting the protein associated with diabetes, making it a leading candidate for further exploration as an antidiabetic agent. Additionally, L7's ligand efficiency (−0.36) was one of the highest in the study, reflecting efficient utilization of its molecular mass in binding with the target protein [7]. L7 (6-(4-sulfophenyl)octanoic acid) likely exhibits a stronger affinity for the target protein than L8 (Empagliflozin) due to its linear structure, which allows better accommodation in hydrophobic binding pockets. L7's 7-carbon alkyl chain enhances hydrophobic interactions, while its carboxylic and sulfonic acid groups enable strong ionic and hydrogen bonding with charged or polar residues on the protein [16–19]. In contrast, L8's bulky cyclohexane structure and multiple hydroxyl groups may hinder effective binding, as they could restrict complementarity with the protein's binding site [16–19]. Overall, L7's combination of optimal hydrophobicity and functional interaction capabilities makes it more favorable for protein binding compared to L8.

L1 (8-Prenylnaringenin) also performed well in the docking study, with a binding energy of −6.92 kcal/mol and an inhibition constant of 8.43 μM. These values are slightly better than Empagliflozin's binding energy (−6.82 kcal/mol) and inhibition constant (10.04 μM), indicating that L1 has comparable or even superior binding affinity [8]. L1's structural characteristics likely contribute to its efficient binding with the protein, making it another strong candidate for further investigation.

Table 2
The results of in silico molecular docking of the selected metabolites with the 7VSI target.

Ligand	Intermol energy (kcal/mol)	Binding Energy (kcal/mol)	Vdw_hb_desolv_energy (kcal/mol)	Inhibition constant (μM)	Ligand efficiency
L1, 8-Prenylnaringenin	−8.71	−6.92	−8.6	8.43	−0.22
L2, 5,6,2′-Trimethoxyflavone	−7.51	−6.32	−7.52	23.25	−0.27
L3, Emodic acid	−7.97	−6.48	−7.51	17.71	−0.29
L4, (8,8-dimethyl-2,10-dioxo-*9H*-pyrano[2.3-*f*]chromen-9-yl) *(Z)*-2-methylbut-2-enoate	−8.0	−7.71	−8.14	6.19	−0.28
L5, (*2S*)-7-hydroxy-2-(4-hydroxyphenyl)-2.3-dihydrochromen-4-one	−7.63	−6.74	−7.27	11.56	−0.35
L6: 5,7-dihydroxy-2-(2,3,4-trihydroxyphenyl)chromen-4-one	−8.0	−6.21	−7.39	27.92	−0.28
L7: 6-(4-sulfophenyl)octanoic acid	−10.27	−7.29	−10.04	4.54	−0.36
L8: Empagliflozin (Reference antidiabetic drug)	−9.8	−6.82	−9.56	10.04	−0.24

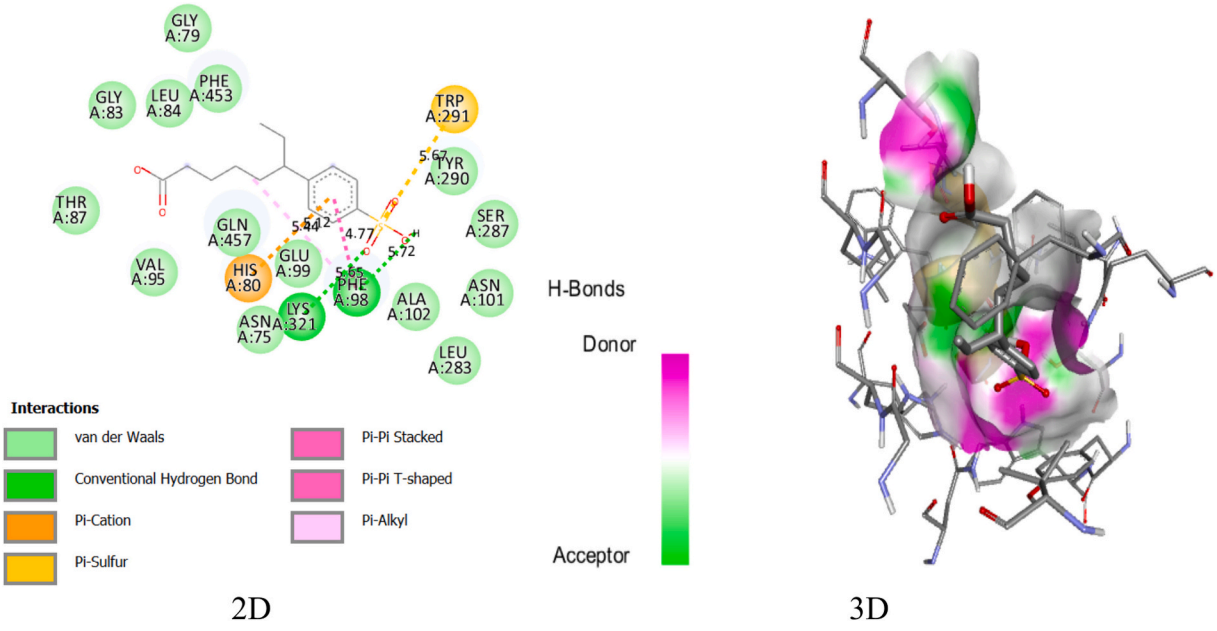

Fig. 3. The best docking complex showing 2D and 3D interactions of the L7 (6-(4-sulfophenyl)octanoic acid) metabolite with the 7VSI receptor.

The presence of multiple functional groups, including hydroxyl groups and a keto oxygen, allows for multiple hydrogen bonding and hydrophobic interactions with the target protein. Additionally, the phenolic structure enhances pi-stacking interactions, promoting stability in the binding pocket [20,21]. The double bond and methyl groups may also facilitate conformational flexibility, allowing L1 to adapt optimally to the binding site [22]. Overall, these features enhance molecular complementarity, leading to a stronger binding affinity than Empagliflozin, which has a less diverse functional group profile and may result in weaker interactions.

Another promising ligand, L4, showed strong binding energy (−7.71 kcal/mol) and an inhibition constant of 6.19 μM. This indicates better binding and inhibition properties than Empagliflozin, further positioning L4 as a competitive alternative for antidiabetic therapy. The compound's van der Waals, hydrogen bond, and desolvation energy profile (−8.14 kcal/mol) supports the stability and specificity of the interaction with the target protein, making it a high-potential candidate for future studies [23]. The strong binding energy of ligand L4 (−7.71 kcal/mol) compared to Empagliflozin ((−6.82 kcal/mol)) can be attributed to its molecular structure, which enables optimal interaction with the target protein. L4 features three keto groups that enhance hydrogen bonding capability, a double bond for increased conformational flexibility, and strategically positioned *trans*-methyl groups that may contribute to steric fitting within the binding site. The presence of three ether oxygen atoms also helps in solvation interactions [24–26]. These structural characteristics facilitate stronger van der Waals interactions and a favorable desolvation energy profile (−8.14 kcal/mol), promoting both stability and specificity in binding, thus positioning L4 as a competitive candidate for antidiabetic therapy.

Other metabolites, such as L3 and L6, showed moderate docking scores. While their binding energies were relatively strong (−6.48 kcal/mol and − 6.21 kcal/mol, respectively), their higher inhibition constants (17.71 μM and 27.92 μM) suggest that they are less potent inhibitors compared to Empagliflozin and other top-performing ligands [27]. Although these metabolites may not be as promising as L7 or L1, their interactions with the target protein should not be entirely discounted and may warrant further optimization for improved efficacy. Overall, the results highlight that L7, L1, and L4 exhibit binding affinities and inhibition constants that surpass or are comparable to those of Empagliflozin, making them strong candidates for further in vitro and in vivo studies. The dual presence of strong binding and efficient inhibition in these metabolites underscores their potential as antidiabetic agents,

and their further development could lead to more effective therapies for diabetes management. Additionally, the insights gained from this study can inform future research into the structure-activity relationships of these metabolites, guiding the design of even more potent antidiabetic drugs.

3.2. Molecular dynamics (MD) analysis

MD simulations and free energy calculations were performed to substantiate the in silico molecular docking results in the current study. The results are shown in Table S3, Table S4, and Fig. S2. Table S3 provides a comprehensive analysis and ranking of the ligands based on both simulated docking scores and MM-PBSA binding free energies. The ranking combines both metrics, with lower (more negative) values indicating stronger predicted binding. Table S3 also ranks the ligands from best (1) to worst (5) overall. The reference drug (empagliflozin) ranks marginally better, demonstrating the strongest predicted binding, followed closely by (2*S*)-7-hydroxy-2-(4-hydroxyphenyl)-2,3-dihydrochromen-4-one (L5) and emodic acid (L3). This suggests these compounds are the most promising for SGLT2 inhibition.

Table S4 presents RMSD (Root Mean Square Deviation) trajectories showing the stability of each protein-ligand complex during the simulation. All three best complexes demonstrate good stability after an initial equilibration period, with RMSD values stabilizing around 2–3 Å, which is typical for well-behaved protein simulations [28,29]. RMSD analysis was performed to assess the overall stability of the protein-ligand complexes during the simulation. The RMSD plot (Fig. S2) indicate that all three top ligands (Reference, (2*S*)-7-hydroxy-2-(4-hydroxyphenyl)-2,3-dihydrochromen-4-one, and emodic acid) maintained stable trajectories, with average RMSD values around 2.2–2.3 Å, suggesting that the complexes remained structurally stable throughout the 100 ns simulation [30].

MD simulation analysis shows that, unlike the in silico molecular docking analysis, which indicated that L7 among other ligands was the best ligand compared to the reference drug empagliflozin, the reference drug exhibited slightly better dynamic behavior compared to the other ligands, with only L3 performing comparably to the reference drug.

Table 3
ADMET results of the seven metabolites of *A. antunesiana* and the reference drugs, Empagliflozin.

Admet Properties	Selected metabolites							Reference Drug
	L1	L2	L3	L4	L5	L6	L7	L8 (Empagliflozin)
Size (MW) g/mol	340.37	312.32	300.22	342.34	256.25	302.24	300.37	450.91
Solubility Log S (ESOL)	−4.91	−3.97	−3.22	−4.08	−3.28	−3.55	−3.12	−3.80
Saturation Fraction Csp3	0.25	0.17	0.00	0.32	0.13	0.00	0.50	0.48
Flexibility (Num. rotatable bonds)	3	4	1	3	1	1	8	6
Num. H-bond acceptors	5	5	7	6	4	7	5	7
Num. H-bond donors	3	0	4	0	2	5	2	4
Molar refractivity	95.29	87.40	72.78	91.55	69.55	78.03	76.69	113.41
Polarity TPSA (Å2)	86.99	57.90	132.13	82.81	66.76	131.36	100.05	108.61
XLOGP3	4.45	3.09	1.88	3.20	2.30	2.17	2.74	2.03
iLOGP	2.76	3.10	0.93	2.71	1.73	1.64	1.83	3.18
WLOGP	3.69	3.49	1.28	3.02	2.48	1.99	4.15	1.29
MLOGP	1.82	1.25	−0.24	1.76	1.27	−0.56	2.56	0.70
SILICOS-IT	3.75	4.08	1.48	3.76	2.55	1.54	2.04	2.66
Lipophilicity average	3.29	3.00	1.07	2.89	2.07	1.36	2.66	1.97
Lipinski	Yes; 0 violation	Yes; 0 violation	Yes; 0 violation	Yes; 0 violation	Yes; 0 violation	Yes; 0 violation	Yes; 0 violation	Yes; 0 violation
Ghose	Yes	Yes	Yes	Yes	Yes	Yes	Yes	Yes
Veber	Yes	Yes	Yes	Yes	Yes	Yes	Yes	Yes
Egan	Yes	Yes	No; 1 violation: TPSA>131.6	Yes	Yes	Yes	Yes	Yes
Muegge	Yes	Yes	Yes	Yes	Yes	Yes	Yes	Yes
Bioavailability score	0.55	0.55	0.56	0.55	0.55	0.55	0.56	0.55
Gastrointestinal (GI) absorption	High	High	High	High	High	High	High	High
Blood brain barrier (BBB) permeability	No	Yes	No	No	Yes	No	No	No
P-gp substrate	No	No	No	No	Yes	No	No	Yes
CYP1A2 inhibitor	Yes	Yes	No	No	Yes	Yes	No	No
CYP2C19 inhibitor	No	Yes	No	Yes	Yes	No	No	No
CYP2C9 inhibitor	Yes	Yes	No	Yes	No	No	No	No
CYP2D6 inhibitor	Yes	Yes	No	No	No	Yes	No	Yes
CYP3A4 inhibitor	Yes	Yes	No	Yes	No	Yes	No	No
Log Kp (skin permeation) cm/s	−5.22	−6.01	−6.80	−6.12	−6.23	−6.60	−6.19	−7.61
Pan assay interference compounds (PAINS)	0 alert	0 alert	1 alert: quinone_A	0 alert	0 alert	1 alert: catechol_A	0 alert	0 alert
Brenk	1 alert: isolated_alkene	0 alert	0 alert	2 alerts: cumarine, michael_acceptor_1	0 alert	1 alert: catechol	1 alert: sulfonic_acid_2	0 alert
Leadlikeness	No; 1 violation: XLOGP3 > 3.5	Yes	Yes	Yes	Yes	Yes	No; 1 violation: Rotors>7	No; 1 violation: MW > 350
Synthetic accessibility	3.67	3.46	2.66	4.09	2.95	3.12	2.79	4.87

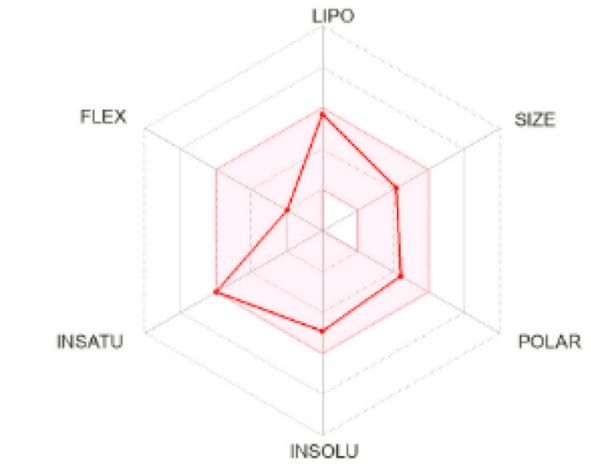

L1_8-Prenylnaringenin

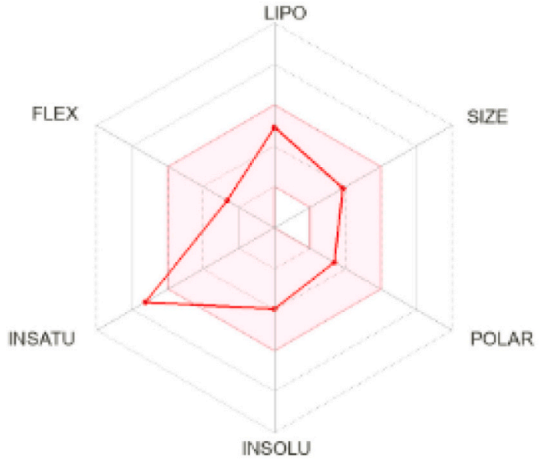

L2_5,6,2'-Trimethoxyflavone

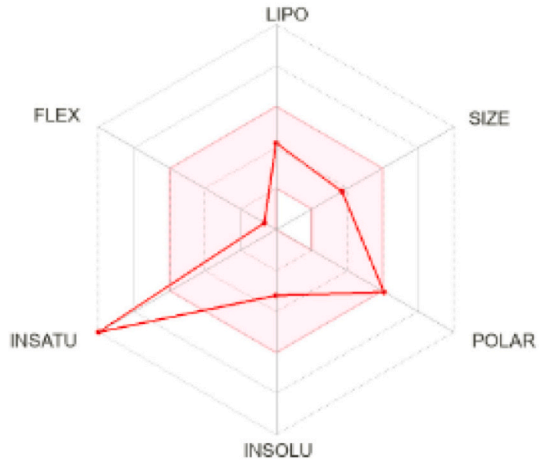

L3_Emodic acid

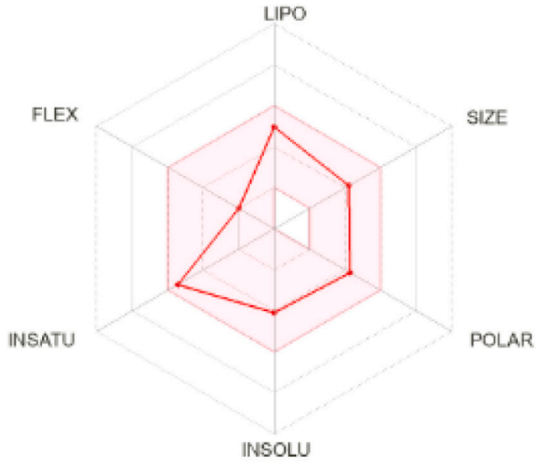

L4_(8,8-dimethyl-2,10-dioxo-*9H*-pyrano[2,3-*f*]chromen-9-yl) *(Z)*-2-methylbut-2-enoate

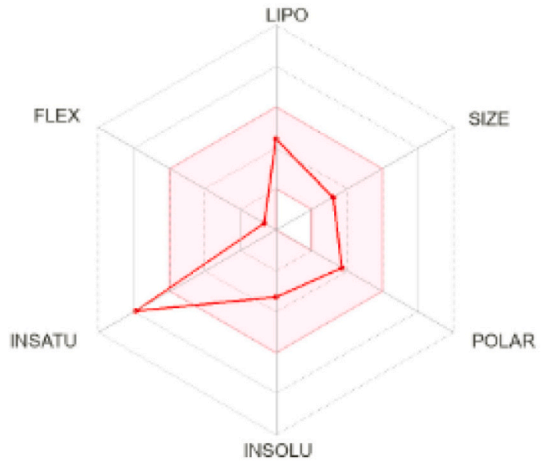

L5_(*2S*)-7-hydroxy-2-(4-hydroxyphenyl)-2,3-dihydrochromen-4-one

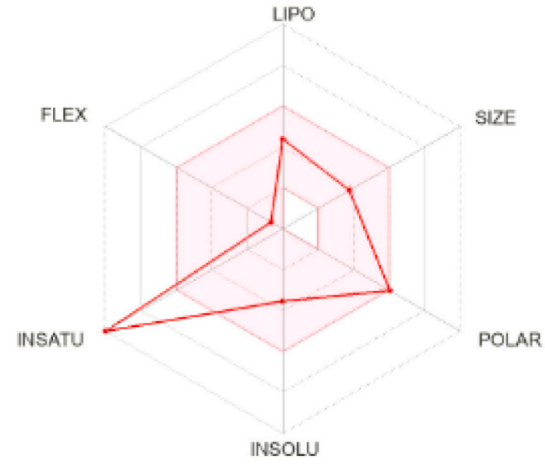

L6_5,7-dihydroxy-2-(2,3,4-trihydroxyphenyl)chromen-4-one

Fig. 4. Bioavailability Radar for the relevant metabolites and the reference drug, Empagliflozin.

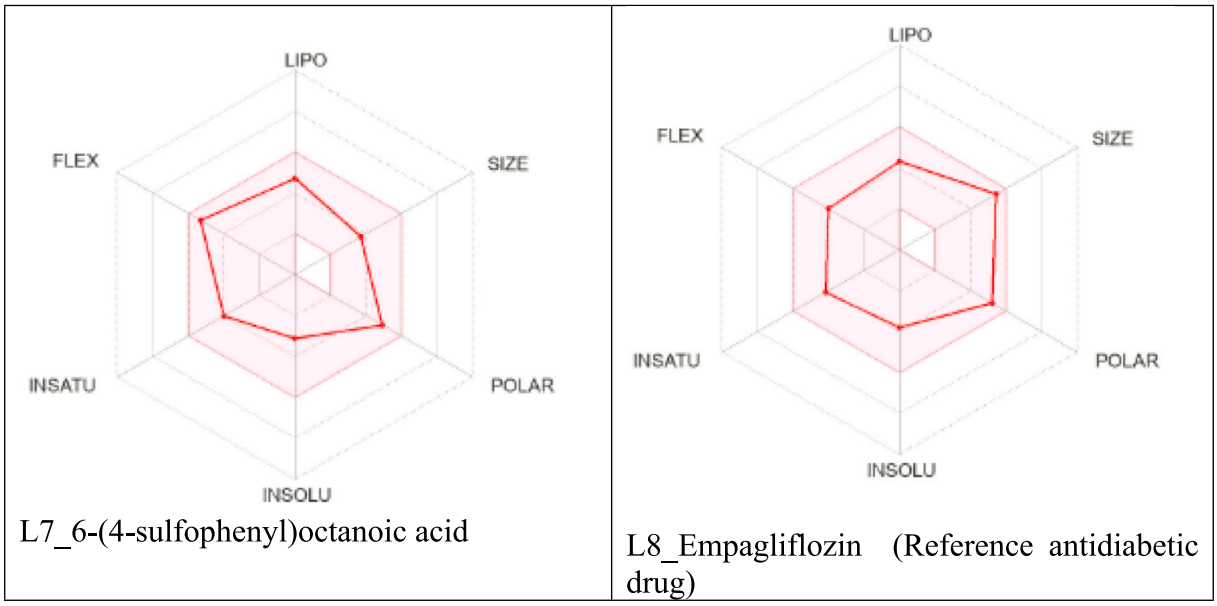

Fig. 4. (*continued*).

3.3. ADMET analysis

Table 3 shows ADMET results of the seven metabolites from the root of *A. antunesiana* and the reference drug; Empagliflozin, whereas Fig. 4 shows the Bioavailability Radar for the relevant metabolites and the reference drug. Fig. 4 particularly illustrates six key physicochemical parameters that are taken into account: saturation, flexibility, solubility, lipophilicity, polarity, and size. For a compound to be considered "drug-like," it must fall within the pink region defined by the characteristics represented on each axis [8]. The ADMET properties for seven metabolites (L1 to L7) of *A. antunesiana* and reference antidiabetic drug, Empagliflozin, were evaluated to understand their potential as therapeutic agents. The ADMET results provide valuable insights into the drug-likeness and pharmacokinetic properties of the selected metabolites from *A. antunesiana* compared to Empagliflozin.

3.3.1. Lipophilicity and solubility

The lipophilicity profiles of the selected metabolites indicate moderate values overall, with L1 (3.29) and L7 (2.66) exhibiting the highest average scores, suggesting that these metabolites are more lipophilic than Empagliflozin (1.97). Metabolites with high lipophilicity may face challenges in absorption and distribution due to poor aqueous solubility [31,32]. Although all metabolites maintained acceptable solubility values, Empagliflozin's solubility score (Log S of −3.80) suggests superior aqueous solubility, potentially enhancing its bioavailability in physiological environments compared to the tested metabolites. Notably, L1 exhibited the lowest solubility (Log S of −4.91), which could limit its therapeutic efficacy unless optimized.

3.3.2. Molecular size, flexibility, and membrane permeability

Molecular weight and flexibility are key indicators of molecular interaction and binding efficacy, with highly flexible compounds often demonstrating improved binding adaptability [33]. Empagliflozin has the highest molecular weight (450.91 g/mol), and is flexible (6 rotatable bonds), contributing to its pharmacokinetic stability. Among the metabolites, L7, with 8 rotatable bonds, shows the highest flexibility, which may provide advantageous conformational adaptability in diverse binding environments. Polar surface area (TPSA), which influences membrane permeability, is highest in L3 (132.13 $Å^2$) and L6 (131.36 $Å^2$), potentially reducing their oral bioavailability [34]. In contrast, Empagliflozin's TPSA (108.61 $Å^2$) falls within a favorable range, enhancing its ability to permeate cellular membranes effectively.

3.3.3. Drug-likeness and rule compliance

All metabolites, along with Empagliflozin, adhere to the Lipinski, Ghose, Veber, Egan, and Muegge rules, signifying strong drug-likeness potential [35,36]. However, L3 violates the Egan rule due to its higher TPSA, and L7 and Empagliflozin demonstrate lead-likeness violations based on the number of rotatable bonds and molecular weight, respectively. These findings indicate that most metabolites could achieve good drug-likeness but may require further optimization for better lead-likeness, particularly concerning molecular size and flexibility [28].

3.3.4. Gastrointestinal absorption and blood-brain barrier permeability

All selected metabolites show high gastrointestinal (GI) absorption, which is critical for oral bioavailability [37–39]. This characteristic is an advantage in potential therapeutic use as orally administered drugs. Among the selected metabolites, L2, and L5 are predicted to cross the blood-brain barrier (BBB), indicating possible central nervous system (CNS) effects [8,40]. This trait can be either a therapeutic advantage or a safety concern, depending on the intended application and the specific target organ. Further evaluation may be required to assess CNS involvement if these metabolites are considered for systemic therapies.

3.3.5. Metabolizing enzyme inhibition and drug-drug interaction potential

Metabolizing enzyme inhibition analysis shows that some metabolites have the potential to inhibit cytochrome P450 enzymes, especially L1 and L2, which inhibit multiple enzymes such as CYP1A2, CYP2C9, and CYP3A4. Inhibiting these enzymes could impact metabolic pathways, creating a potential for drug-drug interactions [41,42]. Empagliflozin, however, demonstrates selective inhibition of CYP2D6, which may limit such interactions. The selective enzyme inhibition observed with Empagliflozin is generally favorable, as it minimizes the risk of unintended metabolic interference.

3.3.6. Toxicity and synthetic accessibility

Regarding toxicity alerts, L3 and L6 present one PAINS alert each due to their quinone and catechol structures, respectively, which may pose a risk of non-specific binding or toxicity [43]. Empagliflozin shows no PAINS or Brenk alerts, highlighting its superior medicinal chemistry profile in terms of safety [44]. L7, with two Brenk alerts (including sulfonic acid), suggests some safety concerns. The synthetic accessibility

scores suggest that L3 is the easiest to synthesize (2.66), while Empagliflozin has a relatively high synthetic accessibility score (4.87), indicating its complex structure and potentially higher production costs [45,46].

The findings indicate that several metabolites exhibit promising ADMET profiles, with L7 emerging as a compound with high flexibility, oral absorption, and good pharmacokinetic attributes, though its reactivity may require further investigation. L1 and L4 also display favorable drug-likeness properties. Empagliflozin, serving as the reference, demonstrates an optimal balance of pharmacokinetic attributes, fewer drug-drug interaction risks, and a safer profile overall, though its complex synthesis could present a manufacturing challenge. Future optimization efforts for these metabolites, along with in vitro testing, are essential to address the identified risks and improve the therapeutic potential of *A. antunesiana* metabolites in antidiabetic applications.

4. Predicted toxicity

4.1. Toxicity predictions for antidiabetic drug candidates and reference drug

ProTox-II is an essential tool in the process of drug design and development because it can predict the toxicities of small metabolites. In the current study, many criteria, including LD50, predicted hepatotoxicity, neurotoxicity, nephrotoxicity, respiratory toxicity, cardiotoxicity, carcinogenicity, immunotoxicity, mutagenicity, cytotoxicity, clinical toxicity, and nutritional toxicity were taken into account for the toxicity analysis. Table 4 shows toxicity analysis of metabolites (L1 to L7) and the reference antidiabetic drug, Empagliflozin.

In a nutshell, L2, L3, and L6 appear to show lower overall toxicity risks compared to the others, but they still present some challenges, particularly regarding nephrotoxicity and respiratory toxicity. L4, although having the lowest LD50 (indicating higher toxicity), shows an inactive profile for key toxicities like nephrotoxicity and hepatotoxicity. Empagliflozin, despite showing risks for nephrotoxicity and cardiotoxicity, maintains a safer overall profile compared to some of the metabolites, especially L1 and L7, which present higher toxicity risks in multiple areas. Further in vivo toxicity testing is necessary to validate these predictions before considering any of these metabolites for therapeutic use.

4.2. Toxicity profile and LD50 analysis

The predicted LD50 values suggest that most of the metabolites, particularly L2 (4000 mg/kg), L3 (5000 mg/kg), and L6 (4000 mg/kg), exhibit lower toxicity risks, falling into toxicity class 5. L1 (2000 mg/kg), L4 (832 mg/kg), and L7 (1653 mg/kg) have relatively lower LD50 values and are categorized in class 4, indicating higher toxicity levels [7,47,48]. Empagliflozin (3000 mg/kg), though in class 5, still presents a moderate toxicity profile, which is a benchmark for evaluating other candidates.

4.3. Organ toxicity

It is vital to ascertain the safety of a drug candidate to avoid organ toxicity [49–51] [29–31]. Both the docking and ADME results highlight that L1 and L4 had strong binding interactions and relatively high lipophilicity. However, they also demonstrated potential nephrotoxicity and moderate hepatotoxicity risks, which could limit their therapeutic potential. Although Empagliflozin showed higher nephrotoxicity (0.93 probability), its inactive hepatotoxicity profile makes it somewhat safer in this regard. In contrast, L2 and L3, which had favorable docking scores and ADME properties, showed lower nephrotoxicity predictions (0.51 and 0.69) and were also inactive for hepatotoxicity, making them better candidates from a toxicity standpoint. The neurotoxicity predictions show that all tested metabolites, including Empagliflozin, are likely to be inactive in this regard, which is a positive outcome for CNS safety. However, respiratory toxicity predictions reveal active risks across all candidates (L1–L7), similar to Empagliflozin. This aspect requires careful consideration, particularly since respiratory issues could complicate diabetes management in vulnerable populations.

4.4. Toxicity end points

Toxicity endpoints are specific biological effects or outcomes used to assess the harmful effects of a substance on an organism or a system

Table 4
Toxicity analysis of metabolites (L1 to L7) from *A. antunesiana* and the reference drug, Empagliflozin.

Tested toxicities	Antidiabetic drug candidates							Empagliflozin (Reference antidiabetic drug)
	L1	L2	L3	L4	L5	L6	L7	L8
Predicted LD50 (mg/kg)	2000	4000	5000	832	2000	4000	1653	3000
Predicted toxicity class	4	5	5	4	4	5	4	5
Hepatotoxicity (prediction/ probability)	Inactive/ 0.69	Inactive/ 0.69	Inactive/ 0.66	Inactive/ 0.63	Inactive/ 0.64	Inactive/ 0.69	Inactive/ 0.66	Inactive/0.75
Neurotoxicity (prediction/ probability)	Inactive/ 0.79	Inactive/ 0.74	Inactive/ 0.87	Inactive/ 0.77	Inactive/ 0.85	Inactive/ 0.89	Inactive/ 0.94	Inactive/0.89
Nephrotoxicity (prediction/ probability)	Active/ 0.58	Active/ 0.51	Active/ 0.69	Inactive/ 0.58	Active/ 0.55	Active/ 0.62	Active/ 0.55	Active/0.89
Respiratory toxicity (prediction/ probability)	Active/ 0.79	Active/ 0.57	Active/ 0.75	Active/ 0.55	Active/ 0.77	Active/ 0.83	Active/ 0.55	Active/0.84
Cardiotoxicity (prediction/probability)	Inactive/ 0.98	Inactive/ 0.71	Inactive/ 0.69	Inactive/ 0.66	Inactive/ 0.77	Inactive/ 0.99	Inactive/ 0.63	Active/0.66
Carcinogenicity (prediction/ probability)	Inactive/ 0.69	Inactive/ 0.53	Inactive/ 0.64	Inactive/ 0.54	Active/ 0.50	Active/ 0.68	Inactive/ 0.78	Inactive/0.68
Immunotoxicity (prediction/ probability)	Inactive/ 0.66	Active/ 0.81	Inactive/ 0.96	Active/ 0.90	Inactive/ 0.94	Inactive/ 0.86	Inactive/ 0.99	Inactive/0.58
Mutagenicity (prediction/ probability)	Inactive/ 0.64	Inactive/ 0.69	Inactive/ 0.78	Inactive/ 0.54	Inactive/ 0.74	Active/ 0.51	Inactive/ 0.72	Inactive/0.73
Cytotoxicity (prediction/ probability)	Inactive/ 0.79	Inactive/ 0.82	Inactive/ 0.96	Inactive/ 0.67	Inactive/ 0.61	Inactive/ 0.99	Inactive/ 0.71	Inactive/0.69
Clinical toxicity (prediction/ probability)	Inactive/ 0.59	Inactive/ 0.60	Active/ 0.56	Inactive/ 0.56	Inactive/ 0.52	Inactive/ 0.53	Inactive/ 0.53	Active/0.52
Nutritional toxicity (prediction/ probability)	Active/ 0.62	Active/ 0.59	Inactive/ 0.66	Active/ 0.69	Active/ 0.56	Active/ 0.63	Inactive/ 0.81	Inactive/0.51

[52–54]. These endpoints are critical in toxicological studies to determine the safety profile of chemical compounds, pharmaceuticals, or environmental substances. Toxicity endpoints help identify the type, severity, and probability of adverse effects that may arise from exposure to a substance. For carcinogenicity, most metabolites, especially L2 and L3, showed favorable predictions of inactivity, aligning with profile of Empagliflozin. However, L5 and L6 raised concerns for active carcinogenic potential, which may compromise their safety profile despite favorable docking interactions. Mutagenicity results were similarly favorable, with L6 being the only metabolite showing an active profile, indicating possible genotoxicity risks. The cytotoxicity analysis shows that none of the metabolites, including Empagliflozin, are predicted to cause cellular damage, further supporting their safety for therapeutic use. Clinical toxicity, however, highlights active predictions for L3 and Empagliflozin. Given that L3 also had favorable docking and ADME results, further in vivo toxicity testing is required to fully understand its clinical impact.

4.5. Best drug candidates

Based on the comprehensive analysis, L2 and L3 emerge as the most promising candidates. They demonstrate:

1. Favorable docking results: Moderate binding energies and inhibition constants.
2. Favorable ADME properties: Both show high GI absorption and acceptable drug-likeness criteria.
3. Low toxicity profiles: Particularly, low risks for nephrotoxicity, hepatotoxicity, and carcinogenicity, along with favorable LD50 values.

While metabolites such as L1 and L4 had stronger docking interactions, their higher toxicity risks, especially in nephrotoxicity and respiratory toxicity, reduce their potential for further development.

It may suffice to emphasize that **L2 and L3** are the most viable antidiabetic drug candidates when compared to Empagliflozin, warranting further investigation for their clinical use. However, given Empagliflozin's extensive clinical validation and moderate toxicity profile, these metabolites would still require in-depth pharmacological and in vivo safety studies before they could be considered for therapeutic application.

5. Conclusions

This study provides a comprehensive evaluation of seven metabolites from *Albizia antunesiana* as potential antidiabetic agents, comparing them to Empagliflozin through molecular docking, ADME, and toxicity analyses. Docking results identified L1, L4, and L7 as having strong binding affinities, while ADME results showed favorable drug-likeness and high gastrointestinal absorption for most metabolites. Toxicity analysis highlighted L2 and L3 as the safest candidates, with low toxicity risks. Overall, L2 and L3 stand out as promising antidiabetic drug candidates, with further investigation warranted for their development. Future research should prioritize in vivo studies to validate the efficacy and safety of L2 and L3 in diabetic models. Additionally, conducting molecular dynamics simulations and free energy calculations showed good dynamic behavior of the reference drug and L3. Exploring the mechanisms of action of these metabolites in future studies will further elucidate their therapeutic potential. Finally, investigating the pharmacokinetics of L2 and L3 in clinical settings could yield valuable insights into their effectiveness and application.

CRediT authorship contribution statement

Bitwell Chibuye: Writing – original draft, Software, Resources, Project administration, Methodology, Investigation, Funding acquisition, Formal analysis, Data curation, Conceptualization. **Indra Sen Singh:** Writing – review & editing, Validation, Methodology, Conceptualization. **Luke Chimuka:** Validation, Resources, Methodology, Funding acquisition. **Mokgaetji Monyai:** Visualization, Validation, Methodology. **Maseka Kenneth Kakoma:** Resources, Conceptualization.

Declaration of competing interest

The authors declare that they have no known competing financial interests or personal relationships that could have appeared to influence the work reported in this paper.

Acknowledgments

The authors sincerely express their gratitude for the assistance provided by the Ministry of Education of the Republic of Zambia, Copperbelt University – Africa Centre of Excellence in Sustainable Mining (CBU – ACESM), University of the Witwatersrand, and Mukuba University, as this study would not have been possible without their support. These institutions had no involvement in the study's design, data collection, analysis, or interpretation; in writing the report; or in deciding to submit the article for publication.

Appendix A. Supplementary data

Supplementary data to this article can be found online at https://doi.org/10.1016/j.rechem.2025.102422.

Data availability

Data will be made available on request.

References

[1] O.E. Adurosakin, E.J. Lweala, J.O. Otike, E.D. Dike, M.E. Uche, J.I. Owanta, O. C. Ugbogu, S.N. Chinedu, E.A. Ugbogu, Ethnomedicinal uses, phytochemistry, pharmacological activities and toxicological effects of Mimosa pudica- a review, Pharmacol. Res. - Modern Chin. Med. 7 (2023) 1–18, https://doi.org/10.1016/j.prmcm.2023.100241.

[2] S.A. Antar, N.A. Ashour, M. Sharaky, M. Khattab, N.A. Ashour, R.T. Zaid, E.J. Roh, A. Elkamhawy, A.A. Al-Karmalawy, Diabetes mellitus: classification, mediators, and complications; a gate to identify potential targets for the development of new effective treatments, Biomed. Pharmacother. 168 (2023) 1–125, https://doi.org/10.1016/j.biopha.2023.115734.

[3] M. Mehndiratta, E.A. Almeida, D. Chawla, S.V. Madhu, S. Garg, R. Kar, Higher oxidative stress and inflammation in obese compared to lean patients with type 2 diabetes mellitus, Aspects of Molecular Medicine 3 (2024) 1–6, https://doi.org/10.1016/j.amolm.2024.100042.

[4] B. Chibuye, I.S. Singh, L. Chimuka, K.K. Maseka, Phytochemical and LCMS/MS Screening, Total Phenolic and Flavonoid Content and Antioxidant Activity of the Leaves of Diospyros batokana (Ebenaceae), Systematic Review Pharmacy 14 (2) (2023) 105–112. Sysrevpharm.org/articles/phytochemical-and-lcmsms-screening-total-phenolic-and-flavonoid-content-and-antioxidant-activity-of-the-leaves-of-diospy.pdf.

[5] B. Chibuye, I.S. Singh, L. Chimuka, K.K. Maseka, Metabolite profiling, phytochemical studies, heavy metal determination and health risk assessment of Entandrophragma delevoyi De wild in Zambia, S. Afr. J. Bot. 172 (2024) 663–677, https://doi.org/10.1016/j.sajb.2024.07.053.

[6] T. Rouquet, M.S. Bonnet, C. Pierre, M. Dallaporta, J.D. Troadec, J. Roux, B. Bariohay, The central question of type 2 diabetes, Pharm Pat Anal 2 (3) (2013) 399–427, https://doi.org/10.4155/ppa.13.22.

[7] B. Chibuye, I.S. Singh, L. Chimuka, K.K. Maseka, In silico and ADMET molecular analysis targeted to discover novel anti-inflammatory drug candidates as COX-2 inhibitors from specific metabolites of Diospyros batokana (Ebenaceae), Biochem Biophys Rep 39 (2024) 1–13, https://doi.org/10.1016/j.bbrep.2024.101758.

[8] R. Mazumder, D. Choudhury, A. Sarkar, A. Ghosh, S. Debnath, B. Debnath, R. Ghosh, In silico approach for identification of potential tetracyclic triterpenoids from mushroom as HMG-CoA reductase inhibitor, Aspects of Molecular Medicine 4 (2024) 100053, https://doi.org/10.1016/J.AMOLM.2024.100053.

[9] A. Kochanowska, P. Rusztyn, K. Szczerkowska, S. Surma, A. Gąsecka, M.J. Jaguszewski, Ł. Szarpak, K.J. Filipiak, Sodium–Glucose Cotransporter 2 Inhibitors to Decrease the Uric Acid Concentration—A Novel Mechanism of Action, J Cardiovasc Dev Dis 2023; 10 (7): 1–18. doi:https://doi.org/10.3390/jcdd10070268.

[10] A.J. Scheen, EMPA-REG OUTCOME: Empagliflozin reduces mortality in patients with type 2 diabetes at high cardiovascular risk, Rev. Med. Liege 70 (2015).
[11] M. Hussain, A. Elahi, J. Iqbal, M. Ghafoor, H. Rehman, S. Akhtar, Comparison of efficacy and safety profile of sodium-glucose Cotransporter-2 inhibitors as add-on therapy in patients with type 2 diabetes, Cureus (2021), https://doi.org/10.7759/cureus.14268.
[12] E. Patorno, A. Pawar, D.J. Wexler, R.J. Glynn, L.G. Bessette, J.M. Paik, M. Najafzadeh, K.G. Brodovicz, A. Déruaz-Luyet, S. Schneeweiss, Effectiveness and safety of empagliflozin in routine care patients: results from the EMPagliflozin compaRative effectIveness and SafEty (EMPRISE) study, Diabetes Obes. Metab. (2022) 24, https://doi.org/10.1111/dom.14593.
[13] A.J. Scheen, Pharmacokinetic and pharmacodynamic profile of empagliflozin, a sodium glucose co-transporter 2 inhibitor, Clin. Pharmacokinet. 70 (11) (2015) 583–589, https://doi.org/10.1007/s40262-013-0126-x.
[14] A. Stalin, K.P. Saravana, K.B. Senthamarai, R. Saravanan, S. Ignacimuthu, Q. Zou, Potential inhibition of SARS-CoV-2 infection and its mutation with the novel geldanamycin analogue: Ignaciomycin, Arab. J. Chem. 17 (2) (2024) 1–16, https://doi.org/10.1016/j.arabjc.2023.105493.
[15] M.S. Musa, M.S. Miah, Y.A. Munni, M.A.M. Patwary, M. Kazi, M.M. Matin, Synthesis and elucidation of strained galactopyronose esters as selective cyclooxygenase-2 inhibitor: a comprehensive computational approach, RSC Adv. 14 (2024) 30469–30481, https://doi.org/10.1039/d4ra03520h.
[16] R. Thevendran, S. Sarah, T.H. Tang, M. Citartan, Strategies to bioengineer aptamer-driven nanovehicles as exceptional molecular tools for targeted therapeutics: a review, J. Control. Release 323 (2020) 530–548, https://doi.org/10.1016/J.JCONREL.2020.04.051.
[17] A.A. Elmaaty, K.M. Darwish, M. Khattab, S.S. Elhady, M. Salah, M.I.A. Hamed, A. A. Al-Karmalawy, M.M. Saleh, In a search for potential drug candidates for combating COVID-19: computational study revealed salvianolic acid B as a potential therapeutic targeting 3CLpro and spike proteins, J. Biomol. Struct. Dyn. 40 (2022), https://doi.org/10.1080/07391102.2021.1918256.
[18] M. Kim, H. Jo, G.Y. Jung, S.S. Oh, Molecular complementarity of Proteomimetic materials for target-specific recognition and recognition-mediated complex functions, Adv. Mater. 35 (2023), https://doi.org/10.1002/adma.202208309.
[19] D. Wang, Q. Guo, Z. Wu, M. Li, B. He, Y. Du, K. Zhang, Y. Tao, Molecular mechanism of antihistamines recognition and regulation of the histamine H1 receptor, Nat. Commun. 15 (2024), https://doi.org/10.1038/s41467-023-44477-4.
[20] Y.S. Muthyalaiah, S. Arockiasamy, A. P. A, Exploring the molecular interactions and binding affinity of resveratrol and calcitriol with RAGE and its intracellular proteins and kinases involved in colorectal cancer, J. Biomol. Struct. Dyn. (2023), https://doi.org/10.1080/07391102.2023.2258993.
[21] H. Guan, W. Zhang, D. Sun-Waterhouse, Y. Jiang, F. Li, G.I.N. Waterhouse, D. Li, Phenolic-protein interactions in foods and post ingestion: switches empowering health outcomes, Trends Food Sci. Technol. 118 (2021) 71–86, https://doi.org/10.1016/J.TIFS.2021.08.033.
[22] M. Amaral, D.B. Kokh, J. Bomke, A. Wegener, H.P. Buchstaller, H.M. Eggenweiler, P. Matias, C. Sirrenberg, R.C. Wade, M. Frech, Protein conformational flexibility modulates kinetics and thermodynamics of drug binding, Nat. Commun. 8 (2017), https://doi.org/10.1038/s41467-017-02258-w.
[23] A.N. Ananda, T. Triawanti, B. Setiawan, A.C. Makati, J.A. Putri, S.J. Raharjo, In silico study of the flavonoid compound of Sauropus androgynus leaves ON RNA-dependent RNA polymerase (RdRp) SARS-CoV-2, Aspects of Molecular Medicine 3 (2024), https://doi.org/10.1016/j.amolm.2023.100032.
[24] X. Du, Y. Li, Y.L. Xia, S.M. Ai, J. Liang, P. Sang, X.L. Ji, S.Q. Liu, Insights into protein–ligand interactions: mechanisms, models, and methods, Int. J. Mol. Sci. 17 (2016), https://doi.org/10.3390/ijms17020144.
[25] D.-W. Zhang, H. Wang, Z.-T. Li, Hydrogen bonding motifs: new progresses, in (2015), https://doi.org/10.1007/978-3-662-45756-6_1.
[26] P. Braun, A.P. Végh, M. Von Jan, B. Strohmann, C.N. Hunter, B. Robert, H. Scheer, Identification of intramembrane hydrogen bonding between 131 keto group of bacteriochlorophyll and serine residue α27 in the LH2 light-harvesting complex, Biochimica et Biophysica Acta (BBA) – Bioenergetics 1607 (2003) 19–26, https://doi.org/10.1016/J.BBABIO.2003.08.004.
[27] H. Hata, D.P. Tran, M.M. Sobeh, A. Kitao, M.M. Sobeh, Binding free energy of protein/ligand complexes calculated using dissociation parallel Cascade selection molecular dynamics and Markov state model, Biophys Physicobiol 18 (2021), https://doi.org/10.2142/biophysico.bppb-v18.037.
[28] M. Sahihi, J. Faraudo, Molecular dynamics simulations of adsorption of SARS-CoV-2 spike protein on polystyrene surface, J. Chem. Inf. Model. 62 (2022), https://doi.org/10.1021/acs.jcim.2c00562.
[29] I. Baruah, G. Borgohain, Temperature dependent molecular dynamics simulation study to understand the stabilizing effect of NADES on the protein β-Lactoglobulin, J. Mol. Graph. Model. 125 (2023) 108582, https://doi.org/10.1016/J.JMGM.2023.108582.
[30] G.G. Abbasova, R.H. Ismayilov, D.B. Tagiyev, H. Şenol, Y. Song, A.A. Medjidov, M. T. Huseynova, P.A. Fatullaeva, P. Taslimi, N. Sadeghian, G.H. Lee, S.M. Peng, Synthesis, characterization, crystal structure, molecular dynamics simulations, MM-GBSA analysis, and bioactivity studies of pyrazine- and pyrimidine-modulated unsymmetrical dipyridylamide complexes, J. Mol. Struct. 1315 (2024) 138896, https://doi.org/10.1016/J.MOLSTRUC.2024.138896.
[31] R. Murugesan, B. Kaleeswaran, In silico drug discovery: Unveiling potential targets in Plasmodium falciparum, Aspects of Molecular Medicine 3 (2024) 100038, https://doi.org/10.1016/J.AMOLM.2024.100038.
[32] S. Preeti, R. Sambhakar, S. Saharan, R. Narwal, V. Malik, A. Gahlot, A. Khalid, K. Najmi, M.A. Zoghebi, M. Halawi, S. Albratty, Mohan, exploring LIPIDs for their potential to improves bioavailability of lipophilic drugs candidates: a review, Saudi Pharmaceutical Journal 31 (2023) 101870, https://doi.org/10.1016/J.JSPS.2023.101870.
[33] A. Basciu, L. Callea, S. Motta, A.M.J.J. Bonvin, L. Bonati, A.V. Vargiu, No dance, no partner! A tale of receptor flexibility in docking and virtual screening, Annu Rep Med Chem 59 (2022) 43–97, https://doi.org/10.1016/BS.ARMC.2022.08.006.
[34] A. Caminero Gomes Soares, G.H. Marques Sousa, R.L. Calil, G.H. Goulart Trossini, Absorption matters: a closer look at popular oral bioavailability rules for drug approvals, Mol. Inform. 42 (2023), https://doi.org/10.1002/minf.202300115.
[35] P. Brandão, C. Marques, A.J. Burke, M. Pineiro, The application of isatin-based multicomponent-reactions in the quest for new bioactive and druglike molecules, Eur. J. Med. Chem. 211 (2021), https://doi.org/10.1016/j.ejmech.2020.113102.
[36] A. AL-Adhreai, M. ALSaeedy, A. Alrabie, I. Al-Qadsy, S. Dawbaa, Z.A.M. Alaizeri, H.A. Alhadlaq, A. Al-Kubati, M. Ahamed, M. Farooqui, Design and synthesis of novel enantiopure Bis(5-Isoxazolidine) derivatives: insights into their antioxidant and antimicrobial potential via in silico drug-likeness, pharmacokinetic, medicinal chemistry properties, and molecular docking studies, Heliyon 8 (2022), https://doi.org/10.1016/j.heliyon.2022.e09746.
[37] A. Kambayashi, Y. Shirasaka, Food effects on gastrointestinal physiology and drug absorption, Drug Metab. Pharmacokinet. 48 (2023) 100488, https://doi.org/10.1016/J.DMPK.2022.100488.
[38] B. Garavaglia, L. Vallino, A. Amoruso, M. Pane, A. Ferraresi, C. Isidoro, The role of gut microbiota, immune system, and autophagy in the pathogenesis of inflammatory bowel disease: molecular mechanisms and therapeutic approaches, Aspects of Molecular Medicine 4 (2024) 100056, https://doi.org/10.1016/J.AMOLM.2024.100056.
[39] H.D. Nguyen, G.H. Vu, W.-K. Kim, Effects of gut microbiota-derived short-chain fatty acids on cognitive impairment: an in-silico study, Aspects of Molecular Medicine 4 (2024) 100047, https://doi.org/10.1016/J.AMOLM.2024.100047.
[40] A.C. Correia, A.R. Monteiro, R. Silva, J.N. Moreira, J.M. Sousa Lobo, A.C. Silva, Lipid nanoparticles strategies to modify pharmacokinetics of central nervous system targeting drugs: crossing or circumventing the blood–brain barrier (BBB) to manage neurological disorders, Adv. Drug Deliv. Rev. 189 (2022) 114485, https://doi.org/10.1016/J.ADDR.2022.114485.
[41] D. Ramsden, E.S. Perloff, A. Whitcher-Johnstone, T. Ho, R. Patel, K.D. Kozminski, C.L. Fullenwider, J.G. Zhang, Predictive in vitro-in vivo extrapolation for time dependent inhibition of CYP1A2, CYP2C8, CYP2C9, CYP2C19, and CYP2D6 using pooled human hepatocytes, human liver Microsomes, and a simple mechanistic static model, Drug Metab. Dispos. 50 (2022), https://doi.org/10.1124/dmd.121.000718.
[42] L.A. Stanley, Drug metabolism, Pharmacognosy: Fundamentals, Applications, and Strategies, Second Edition, 2024, pp. 597–624, https://doi.org/10.1016/B978-0-443-18657-8.00029-3.
[43] J.L. Bolton, T. Dunlap, Formation and biological targets of quinones: cytotoxic versus cytoprotective effects, Chem. Res. Toxicol. 30 (2017), https://doi.org/10.1021/acs.chemrestox.6b00256.
[44] A. Daina, O. Michielin, V. Zoete, SwissADME: a free web tool to evaluate pharmacokinetics, drug-likeness and medicinal chemistry friendliness of small molecules, Sci. Rep. 7 (2017), https://doi.org/10.1038/srep42717.
[45] M. Parrot, H. Tajmouati, V.B.R. da Silva, B.R. Atwood, R. Fourcade, Y. Gaston-Mathé, N. Do Huu, Q. Perron, Integrating synthetic accessibility with AI-based generative drug design, J. Chem. 15 (2023), https://doi.org/10.1186/s13321-023-00742-8.
[46] G. Skoraczyński, M. Kitlas, B. Miasojedow, A. Gambin, Critical assessment of synthetic accessibility scores in computer-assisted synthesis planning, J. Chem. 15 (2023), https://doi.org/10.1186/s13321-023-00678-z.
[47] B. Maarif, M. Aminullah, N.L. Saidah, F.A. Muslikh, A. Rahmawati, Y.Y. A. Indrawijaya, D.P. Sari, M.M. Taek, Prediction of Antiosteoporosis activity of thirty-nine phytoestrogen compounds in estrogen receptor-dependent manner through in silico approach, tropical journal of, Nat. Prod. Res. 5 (2021), https://doi.org/10.26538/tjnpr/v5i10.6.
[48] Belia Bima Nafisa, Sanarto Santoso, Zainabur Rahmah, Roihatul Muti'ah, Potential antiviral activity of eleutherine, isoeleutherine, eleuthinone and elecanacine compounds in Eleutherine palmifolia (L.) Merr against NSP3 SARS-COV-2: In silico study, GSC Biological and Pharmaceutical Sciences 22 (2023). doi:10.30574/gscbps.2023.22.2.0063.
[49] R.P. Pandey, J. Vidic, R. Mukherjee, C.M. Chang, Experimental methods for the biological evaluation of nanoparticle-based drug delivery risks, Pharmaceutics 15 (2023), https://doi.org/10.3390/pharmaceutics15020612.
[50] M. Karabicici, S. Akbari, O. Ertem, M. Gumustekin, E. Erdal, Human liver organoid models for assessment of drug toxicity at the preclinical stage, Endocr. Metab. Immune Disord. Drug Targets 23 (2023), https://doi.org/10.2174/1871530323666230411100121.
[51] S.A. Adelakun, A.J. Akomaye, O.D. Omotoso, O.A. Arowosegbe, Anti-hepatopathy and anti-nephropathy activities of Taraxacum officinale in a rat model of Streptozotocin diabetes-induced hepatorenal toxicity and dyslipidemia via attenuation of oxidative stress, inflammation, apoptosis, electrolyte imbalances, and mitochondrial dysfunction, Aspects of Molecular Medicine 3 (2024) 100034, https://doi.org/10.1016/J.AMOLM.2024.100034.
[52] S. Halappanavar, P. Nymark, H.F. Krug, M.J.D. Clift, B. Rothen-Rutishauser, U. Vogel, Non-animal strategies for toxicity assessment of nanoscale materials: role

of adverse outcome pathways in the selection of endpoints, Small 17 (2021), https://doi.org/10.1002/smll.202007628.

[53] R.N. Prasad, T.J. Royce, F. Chino, R. Jagsi, J.D. Palmer, Financial toxicity as an end point in prospective clinical trials involving radiation therapy, Adv. Radiat. Oncol. 7 (2022), https://doi.org/10.1016/j.adro.2022.100970.

[54] C.N. Cavasotto, V. Scardino, Machine learning toxicity prediction: latest advances by toxicity end point, ACS Omega 7 (2022), https://doi.org/10.1021/acsomega.2c05693.